SUPPLEMENT TO THE *WELDING JOURNAL*, APRIL 2011
Sponsored by the American Welding Society and the Welding Research Council

Filler Metal Influence on Weld Metal Structure of Microalloyed Steel

The impact of changes in filler metal chemical composition and heat input on microstructure and mechanical properties during welding X65 steel was evaluated

BY N. BAJIC, V. SIJACKI-ZERAVCIC, B. BOBIC, D. CIKARA, AND M. ARSIC

ABSTRACT

This paper investigates the impact of the chemical composition of the filler metal and welding parameters on the structure of weld metal and the heat-affected zone (HAZ) of microalloyed steel of increased strength, class Nb/V, mark X65 (according to API 5L standard). Experimental welding of steel strip samples (thicknesses of 9.5, 11.0, and 14.5 mm) was performed by shielded metal arc welding (SMAW), with different welding parameters, using two filler metals of different chemical compositions. Based on the analysis of the structure of the weld metal and the HAZ, the proportion of individual microconstituents was determined in order to select the optimal composition of the filler metal and welding parameters. It was shown that filler metal marked NM1 (1.4% Ni, 0.35% Mo) achieved the optimal microstructure (AF, SF, FS), which was confirmed by testing fracture toughness at low temperatures. It was also shown that finer microstructure in the HAZ area could be achieved at low heat input.

Introduction

The main feature of microalloyed high-strength steel for Class-X tube is a fine-grained ferrite-pearlite structure obtained by thermal-mechanical processing. This structure favorably affects the flow stress and toughness of steel. The basic microalloying element in fine-grained microalloyed steels is niobium in combination with vanadium and titanium (Nb/V, Nb/Ti, and Nb/V/ Ti) (Refs. 1–3).

Weldability of steels depends on the base metal and filler metal, as well as the conditions in which the welded construction was made and the quality of construction. Of all the factors, the base metal has the greatest impact. Mechanical and technological properties of welded joints are directly dependent on the chemical composition (base metal and weld metal) and the structure of the weld metal and the heat-affected zone (HAZ) (Ref. 3).

The microstructure of the weld metal in joints of fine-grained steel consists of three basic modifications of ferrite: needle ferrite (acicular ferrite, AF), polygonal ferrite (primary ferrite, PF), and Widmanstätten ferrite (WF). These modifications occur due to different mechanisms of transformation and differently influence the values of strength and toughness of welded joints. Fine needle ferrite grains are mutually separated by boundaries with high-carbon content. This structure provides maximum resistance to crack development (Refs. 3–5). Depending on the thermal cycle of welding and the chemical composition of the weld metal in the high-temperature field, different morphological modifications of ferrite (primary, lamellar-plate, and needle-acicular) occur. High strength and plasticity in the weld metal of microalloyed steel is achieved by alloying the weld metal with various elements.

The chemical composition of the weld metal is characterized by significantly higher content of oxygen in relation to the chemical composition of steel (Ref. 3). Oxygen influences the transformation of austenite in the weld metal only if it is present in the form of oxide and oxide-sulfide inclusions. With increasing concentration of oxygen, the bainite in the microstructure of the weld metal is replaced by acicular ferrite. If the weld metal has less oxygen in it (which implies a smaller number of inclusions), the length-width ratio of the needles of acicular ferrite increases, which causes a decrease in toughness of weld metal (Ref. 3).

In the process of welding, the speed of metal cooling in the stage of crystallization is determined by the operating power of the welding machine. It was shown (Refs. 1–5) that during welding with low-alloyed weld metal, greater operating power affected the formation of polygonal ferrite within the primary austenite grains. The increase of cooling speed leads primarily to the formation of needle ferrite in the structure.

The structure of the HAZ depends on the properties of the base metal, welding

KEYWORDS

Ferrous Metals
Steel Alloys
Welding
Microstructure

N. BAJIC (ihis@eunet.rs) *and B. BOBIC are with IHIS Research and Development Center, Belgrade, Serbia. V. SIJACKI-ZERAVCIC is Faculty of Mechanical Engineering, Belgrade, Serbia. D. CIKARA is Faculty of Technical Sciences, Kosovska Mitrovica, Serbia. M. ARSIC is with Institute for Testing of Materials, Belgrade, Serbia.*

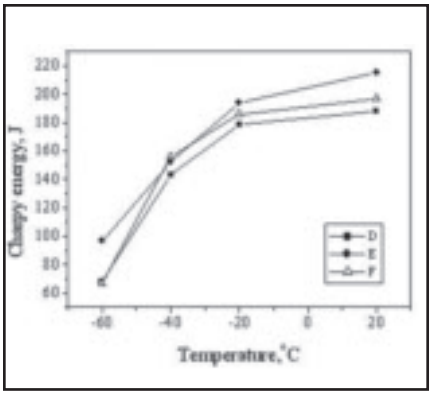

Fig. 1 — Variation in Charpy impact energy depending on temperature for different thicknesses of X65 steel strip: D, t_0 = 9.5 mm; E, t_1 = 11.0 mm; F, t_2 = 14.5 mm.

heat input, and the cooling speed (Refs. 1–5). The width of the HAZ depends on the welding parameters (current intensity, voltage, and welding speed) that are specific to heat input. To select the optimal parameters for welding, it is necessary to monitor the transformation of austenite under the influence of the welding thermal cycle, using the CCT diagram (Ref. 6).

The main criteria for the selection of a filler metal are yield stress, tensile strength, and toughness of the weld metal. Microalloyed steels of increased strength are sensitive to formation of cracks, and it is necessary that the filler metal, in addition to containing elements that improve the properties of the weld metal, contains elements that increase the resistance to the formation of cracks. Elements that are most commonly used for alloying weld metal are Mn, Cr, Ni, and Mo (Refs. 7–12).

The main objective of this study was to assess the impact of changes in chemical composition of the filler metal and the level of heat input during welding microalloyed steel X65 on the improvement of microstructural and mechanical properties of welded joints, especially the toughness at low temperatures.

Experimental Procedure

Materials: Base and Filler Metals

Base metal. Hot-rolled strips of microalloyed steel quality Nb/V mark X65 (according to API-5L) produced in Smederevo plant were chosen for experimental research.

Samples of steel strips were of different thicknesses and were obtained from three batches of microalloyed steel and marked D, E, and F. The chemical compositions of the microalloyed X65 steel from different batches and different thicknesses of steel strips (D, t_0 = 9.5 mm; E, t_1 = 11.0 mm; F, t_2 = 14.5 mm) are given in Table 1.

The results of testing the mechanical properties of the X65 steel strip samples and the calculated values of carbon equivalent (C_{eq}) are given in Table 2.

Samples for mechanical testing were taken perpendicular to the direction of rolling, and the results are expressed as the mean of three tests. Carbon equivalent values are calculated according to the formula $C_{eq} = C + Mn/6 + (Cr + Mo + V)/5 + (Ni + Cu)/15$) (Ref. 5).

Impact values for toughness of the base metal (X65 steel) at different test temperatures are given in Fig. 1.

Filler metal. For experimental welding using the shielded metal arc welding (SMAW) process, coated electrodes intended for welding microalloyed steels were chosen with different chemical compositions. Basic electrodes E8018-C1 (standard AWS A5.5-69) were selected and marked NM1 (alloyed with Ni and Mo), and N1 (alloyed with Ni). Marks of the mentioned electrodes and their size as well as chemical composition and mechanical properties of the weld metal according to the producers catalog are given in Table 3.

Experimental Welding

Preparation of Samples and Welding

Samples for experimental welding were cut from hot-rolled steel strips, so that the longer sample side-plate was in the direction of rolling, and then machine finishing of the sample edges was done.

Dimensions of samples were 300 × 125 × t mm, where t denotes the sample thickness. During welding the following parameters were varied: thickness of steel strip, t_0 = 9.5 mm, t_1 = 11.0 mm, t_2 = 14.5 mm; content of nickel in the electrode, NM1 contains 1.4% while N1 contains 1.10%; content of molybdenum in the NM1 electrode was 0.35%; heat input was varied on two levels for each steel strip thickness as follows: E_1 = 7.3 kJ/cm and E_2 = 18.5 kJ/cm.

Experimental welding of samples in horizontal position was performed continuously by SMAW with LKA-250 device using the welding parameters listed in Table 4. The interpass temperature during welding was controlled by contact thermometer. Experimental welding was performed without preheating the base metal because the calculated values for C_{eq} for all qualities of microalloyed X65 were below the borderline allowance. The number of weld passes for the experimental plates ranged from 5 to 10, and depended on the following factors: the diameter of the electrode, energy parameters, and planned heat input.

Microstructural Analysis of the Weld Metal

Microstructure of the weld metal (obtained with different filler metals and welding parameters) was compared with the expected microstructure that would be obtained according to CCT diagrams for different cooling speeds (Ref. 6). Investigations of the microstructure were performed by optical microscopy (OM) and scanning electron microscopy (SEM).

Microphotographs of characteristic places in the structure of the weld metal are given in Fig. 2A–F. The presence of different morphological forms of ferrite was noticed in the weld metal of all the welded joints. Acicular ferrite (AF), ferrite with a secondary phase (FS), and Widmanstätten ferrite (WF) were mostly found.

The microstructure of the weld metal (using electrode N1 on X65 steel strips) at low heat input consisted mainly of AF. For the smallest thickness of the steel strip (D), the AF was ~ 50%. With increasing thickness (E and F), the AF was lower (~ 35%), while the rest consisted of proeutectoid ferrite (PF) and secondary ferrite (FS) separated at grain boundaries — Fig. 2A, C, E. The expected effects of the nickel influence in forming needle ferrite were realized.

Table 1 — Chemical Composition of Microalloyed Steel X65

Steel Grade	Designation	Chemical Composition*(wt-%)									
		C	Si	Mn	P	S	Al	Cu	Nb	V	N_2
Nb/V	D	0.066	0.179	1.440	0.013	0.006	0.031	0.068	0.039	0.066	0.0099
	E	0.067	0.201	1.490	0.013	0.007	0.028	0.080	0.039	0.065	0.0099
X65	F	0.076	0.231	1.511	0.013	0.004	0.019	0.034	0.037	0.067	0.0103

*Fe is remainder.

In the weld metal microstructure of electrode NM1, about 35% AF was found in the strip of smallest thickness (D). The amount of AF increases with increasing thickness of strips (E and F) and reaches ~ 50%, while the rest consists of FS + SF — Fig. 2B, D, F. The expected effects of nickel in forming needle ferrite in the weld metal were realized, as well as the effect of molybdenum on the optimal relations of structural components.

The obtained results concerning the share of certain microconstituents were compared with the expected shares according to the appropriate CCT diagram. It was concluded that for all the examined samples, satisfactory microstructure was obtained in terms of content of microconstituents (results obtained within the limit values). Some deviation was obvious for the sample thickness D welded by electrode NM1 (Table 5).

Microstructural Analysis of the HAZ

The microstructure of the base metal (steel X65) was fine-grained ferrite-pearlite — Fig. 3A–C. The appearance of the microstructure of the HAZ in the recrystallization zone at the weld interface is shown in Fig. 4A–I. The structure of pretransformed pearlite in the HAZ in the low-temperature zone (A_1 to A_3, according to the Fe-C diagram) depends on the starting structure, which differs in grain size — Fig. 4A–C. The appearance of the HAZ structure in the overheated zone at the weld interface are seen in Fig. 4D–I.

An analysis of the HAZ structure of the welded joints of X65 steel (quality E) along the interface of the base metal to the weld metal was performed, using SEM. The changes in the structure of the HAZ are shown in Fig. 5. A fine-grained ferrite-pearlite structure with small carbides distributed along the grain boundaries is shown in Fig. 5A, and in Fig. 5B, the structure in the recrystallization zone (below A_1), which is finer in relation to the structure of the base metal, is shown. In the precrystallization zone (Fig. 5C), the grain size is nonhomogenous. Untransformed ferrite grains are larger than in the previously observed structure, but the share of pearlite-ferrite structure, which occurred due to austenite transformation, is significantly smaller.

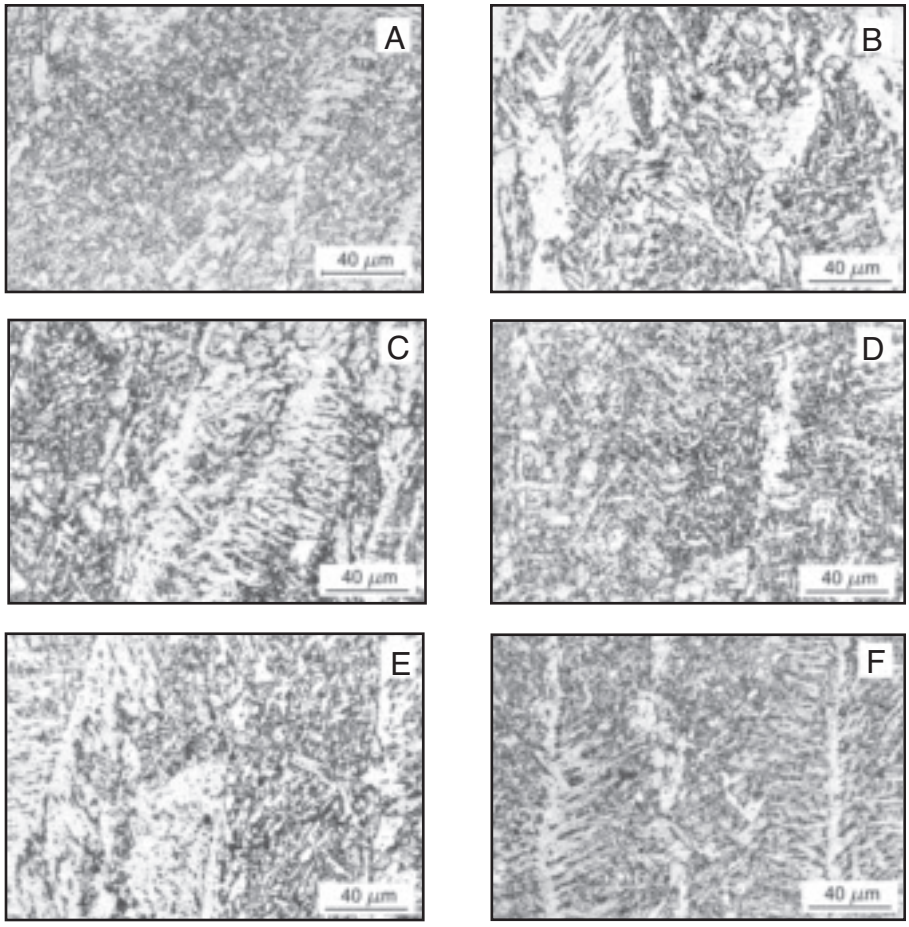

Fig. 2 — Microstructure of weld metal in the last pass. Welding of microalloyed steel X65 strips of different thicknesses (D, E, F) derived by SMAW process with electrodes N1 and NM1.

The appearance of the ferrite-bainite structure formed from the transformation in the area immediately above the A_3 temperature (normalization zone) is shown in Fig. 5D. In the overheated zone (Fig. 5E), a coarse ferrite-bainite structure occurred. Size, shape, and layout of the carbides along the boundaries of former austenite grains can be seen. The appearance of the structure at the weld interface is shown in Fig. 5F.

Table 2 — Mechanical Properties of Microalloyed Steel X65 and Carbon Equivalent C_{eq}

Steel Grade	Designation	Thickness, mm	0.2 YS, MPa	UTS, MPa	0.2 YS/ UTS	E_5, %	Carbon Equivalent C_{eq}
Nb/V	D	9.5	531	619	0.85	35	0.310
	E	11.0	537	635	0.84	35	0.320
X65	F	14.5	456	568	0.80	41	0.330

Table 3 — Basic Mark of Electrodes and Characteristics of the Weld Metal

Designation	Diam. mm	Chemical Composition of Weld Metal (wt-%) C	Si	Mn	Ni	Mo	Mechanical Properties of Weld Metal 0.2 YS, MPa	UTS, MPa	E_5, %	kV, J (–40°C)
NM1	4.0	0.06	0.40	0.90	1.40	0.35	>520	640–710	>22	>125
N1	3.25	0.06	0.5	0.90	1.10	—	>460	570–650	>22	>47

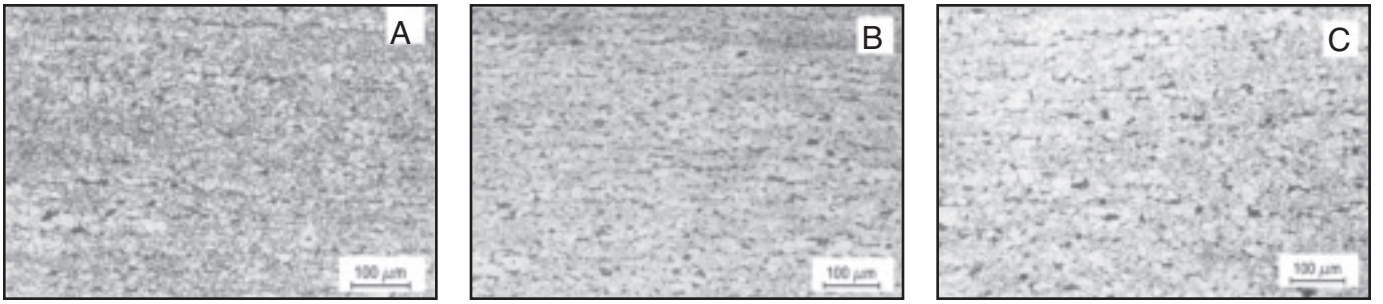

Fig. 3 — Microstructure of base metal (microalloyed steel X65) for different thicknesses of strip: D, t_0 = 9.5 mm; E, t_1 = 11.0 mm; F, t_2 = 14.5 mm.

Fractographic Analysis of the Weld Metal Fracture

After testing fracture toughness of the weld metal at temperatures of +20°, –40° and –60°C, fractographic analyses of the samples were carried out. Welded joints were made by using electrode N1 or NM1. The appearance of fracture surface of the weld metal made by using electrode N1 on microalloyed steel X65 (quality E) is shown in Fig. 6A–F.

The surface of all tested samples indicated the presence of a mixed or typical brittle fracture depending on the test temperature. The weld metal fracture of mixed character was also obtained when testing at –40°C — Fig. 6C, D. Morphological characteristics correspond to the dominant transcrystal brittle fracture that formed by tearing, with a ductile phase around the grains. General appearance of the fracture in the zone that is at the root of the weld metal is shown in Fig. 6C, while the presence of pores and microfractures in the zone of the weld metal face can be observed in Fig. 6D.

The morphological appearance of the characteristic fracture surface of weld metal obtained at –60°C, is shown in Fig. 6E, F. In this case, the fracture is completely of a brittle character (transcrystal and intercrystal). General appearance of the fracture in the middle of the weld metal, which is typically brittle (transcrystal and intercrystal), is shown in Fig. 6E. The transcrystal brittle fracture with microspaces (pores) in the weld metal is presented in Fig. 6F. Figure 7A–F shows the appearance of the fracture surface of the weld metal made with electrode NM1 on X65 steel (quality E, t_1 = 11.0 mm).

Figure 7B shows the appearance of ductile fracture in the middle of the tube (middle of the weld metal). Elongation of dimples in the direction of deformation and partial filling of the dimples with carbide and other particles was noticed.

In the welded joint sample that was broken at –40°C, the fracture surface has a typical appearance of a brittle fracture of transcrystal and intercrystal character. Also, the fracture surface in the middle of the weld metal tested at –40°C shows brittle fracture of transcrystal and intercrystal character — Fig. 7C. Figure 7D shows brittle fracture caused by tearing.

Figure 7E, F shows the fracture surface along the height of weld metal of the sample that was tested at –60°C. The analyzed sample showed brittle fracture caused by tearing — Fig. 7E. Figure 7F shows general appearance of a brittle fracture in the middle of the weld metal.

The results of fractographic analysis of weld metal (using electrode N1) showed that the fracture was mixed (Fig. 6A, B), while in the weld metal (when using electrode NM1), the fracture was ductile on the entire cross section — Fig. 7A, B. The results were obtained at 20°C. The share of brittle fracture in the weld metal when lowering the temperature significantly increases and at –40°C a transcrystal fracture was observed — Fig. 6C, D and 7C, D.

In both groups of samples tested at –60°C, brittle fracture of transcrystal and intercrystal character was clearly observed — Figs. 6E, F and 7E, F. Fractographic analysis has also shown that a more favorable weld metal structure was achieved when using electrode NM1 (1.4% Ni, 0.35% Mo) in relation to the weld metal structure when using electrode N1 (1.0% Ni) at all test temperatures.

Table 4 — Welding Parameters of Microalloyed Steel X65 Samples

Base Metal			Filler Metal		No. of	Energy Parameters			
Steel Grade	Designation	Thickness, mm	Designation	∅ mm	passes	U, V	I, A	V, cm/min	E kJ/cm
Nb/V X65	D	9.5	N1	3.25	6	25	120	17.2	16.8
			N1	3.25	9	25	115	24	6.8
			NM1	4.0	5	25	135	16	12.3
	E	11.0	N1	3.25	9	27	125	26	9.2
			N1	3.25	9	25	118	25	7.3
			NM1	4.0	5	25	140	15	13.7
	F	14.5	N1	3.25	10	25	125	18	10.8
			N1	3.25	4	25	118	19	9.1
			NM1	4.0	7	25	150	17	16.6

Mechanical Properties of Welded Joints

Tensile strength. Results of tensile strength tests of base metal of various thicknesses are given in Fig. 8A, and the results of tensile strength of welded joints are clearly given in Fig. 8B. Tensile strength testing was performed on three samples for each thickness of the steel strip. It was noted that the location of fracture of specimens depended on the thickness of the base metal, as follows: at thickness t = 9.5 mm, the fracture occured in the base metal; at thickness t = 11 mm, the fracture occured in the weld metal; at thickness t = 14.5 mm the fracture occured in the HAZ regardless of the type of filler metal, the number of passes, and the level of heat input during welding.

Hardness. A change of hardness in welded joints depends on the chemical composition of filler metals, welding parameters, and number of passes. In samples of welded joints, hardness measurements were performed in the cross section along the line that runs 2 mm parallel to the weld metal face (L_1), and along the middle of the height of the weld metal (L_s). For certain qualities of base metal and filler metal, change in hardness curves through the welded joint were constructed. Measuring points are shown on the sketch in Fig. 9A–C. A somewhat larger decline of hardness in the HAZ and a larger increase in hardness in the weld metal (in line L_1) in relation to the meas-

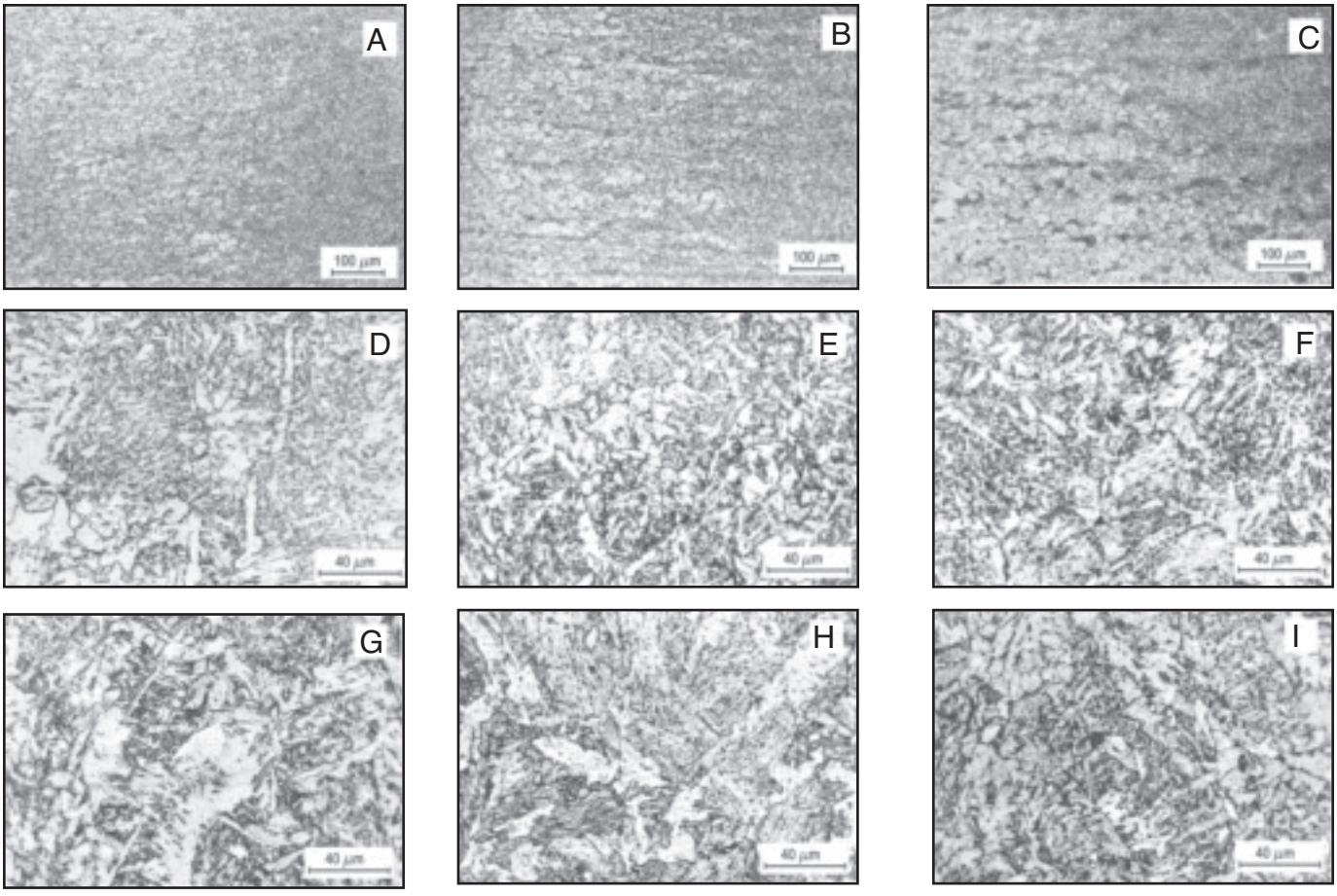

Fig. 4 — Microstructure of HAZ of welded joints of microalloyed steel X65 of different quality (D, E, F). A, B, and C recrystallization and precrystallization zone: A — D, E_1 = 12.3 kJ/cm; B — E, E_2 = 3.7 kJ/cm; C — F, E_3 = 16.6 kJ/cm. D–I weld interface: D — D, E_1 = 6.8 kJ/cm, N1; E — E, E_2 = 9.2 kJ/cm, N1; F — F, E_3 = 10.8 kJ/cm, N1; G — D, E_1 = 12.3 kJ/cm, NM1; H — E, E_2 = 13.7 kJ/cm, NM1; I — F, E_3 = 16.6 kJ/cm, NM1.

uring points that are in the middle of the height of the weld metal (L_s) was observed. In samples of welded joints in steel F, a lower hardness was observed in the HAZ and the weld metal compared to steels D and E. It was also noticed that an increased number of passes had an impact on the reduction of hardness in the weld metal (L_s).

Toughness. The impact test was carried out using the standard Charpy pendulum. The results obtained depending on test temperature are given in Fig. 10A–C. A change of toughness in the weld metal from electrodes N1 and NM1 in steel D, with different levels of heat input is shown in Fig. 10A. Some improvement of toughness was noted at lower temperatures in weld metal from electrode NM1.

Discussion of Results

The results of microstructural examinations and fractographic analyses of weld metal and HAZ of welded joints in steel X65 have shown the impact of filler metals (N1 and NM1) and welding parameters on improving the structure of the weld metal and HAZ. The microstructure of steel X65 is a homogeneous ferrite-pearlite one and strip-like directed toward the rolling direction — Fig. 3A–C. For steel strip thickness of 9.5 mm, the grain size is 11; for thickness of 11.0 mm, the grain size is 9.5; and for thickness of 14.5 mm, the grain size is 9. It can be seen that steel strip

Table 5 — Share of Certain Ferrite Morphologies in Microalloyed Steel X65

Base Metal	D(t_0 = 9.5 mm)		E (t_1 = 11.0 mm)		F (t_2 = 14.5 mm)	
Filler Metal	N1	NM1	N1	NM1	N1	NM1
Line Energy	E_1=6.8 kJ/cm	E_3=16.8 kJ/cm	E_2=9.2 kJ/cm	E_3=13.7 kJ/cm	E_1 =9.1 kJ/cm	E_3+16.6 kJ/cm
Microstructure of Weld Metal	~50% AF remainder PF partially coarse grain in blocks and FS	~35%AF coarse WF and coarse grain PF+FS	~36%AF Rest PF+FS and coarse WS	~50%AF Rest PF+FS and a small amount of WF	~35%AF Rest very coarse PF WF	~50%AF Rest PF+FS+WF
Microstructure CCT diagram	20–48%AF Rest FS	5–75%AF Rest PF+FS+WF	20–48% AF Rest PF+FS+WF	50–75% AF Rest PF+FS+WF	20–48% AF Rest PF+WF	50–75% AF Rest PF+FS+WF

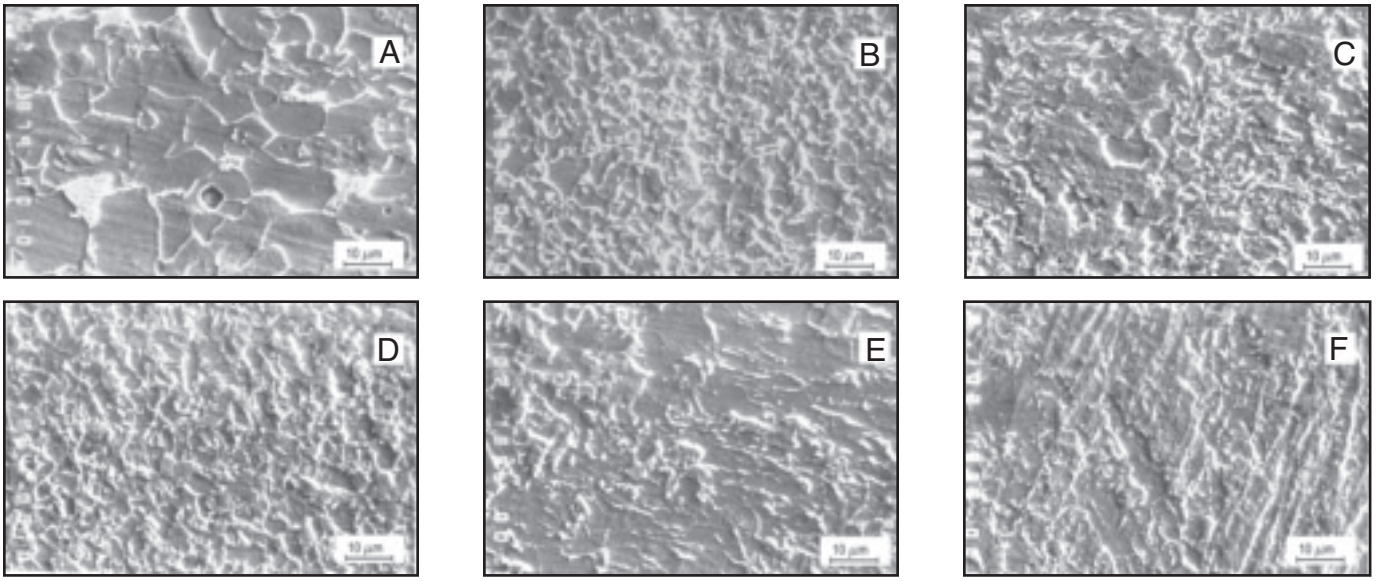

Fig. 5 — SEM, microstructure of HAZ of welded joint of microalloyed steel X65 (quality E, t_1 = 11.0 mm). A — Base metal (ferrite + pearlite); B — normalization zone; C — overheating zone; D — fine-grain zone (ferrite + pearlite); E — overheating zone; F — weld interface (column-like crystals).

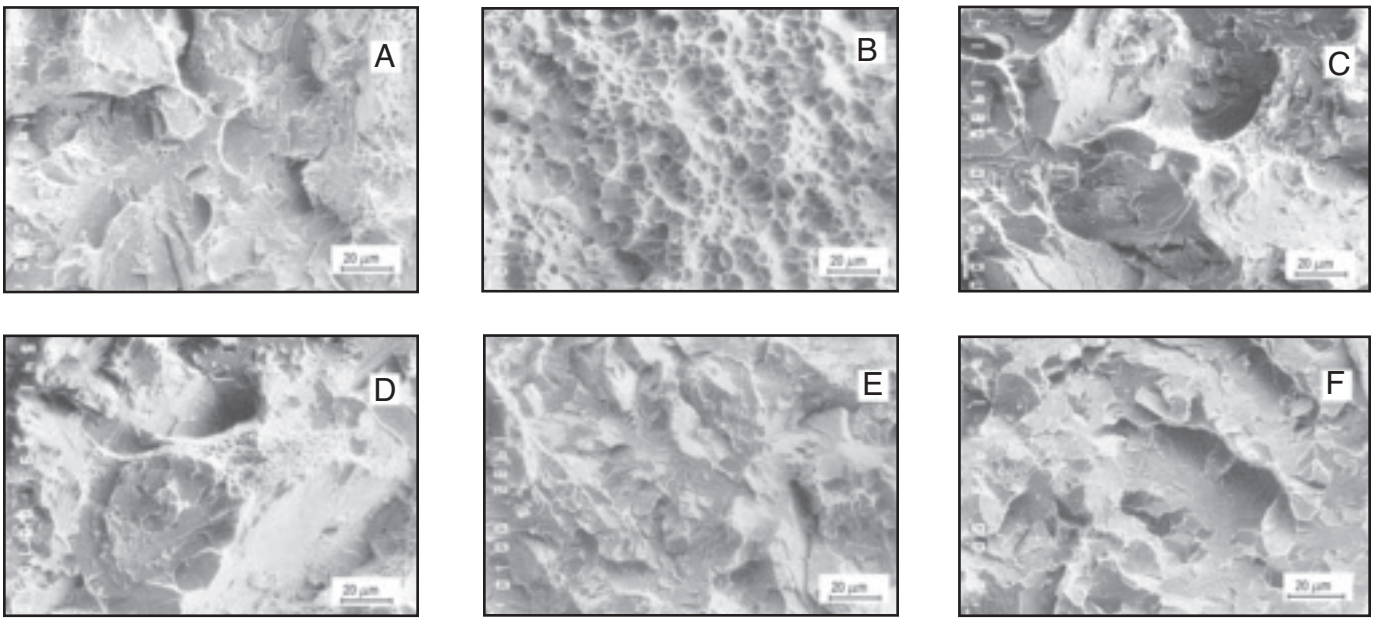

Fig. 6 — SEM, fracture surface of weld metal made by using electrode N1 on microalloyed steel X65 (quality E, t_1 = 11.0 mm). A — Mixed fracture with dominant transcrystal brittle fracture (+20°C); B — ductile fracture with small cavities containing particles of sediment (+20°C); C — transcrystal brittle fracture in the middle of the weld metal (–40°C); D — mixed fracture mainly transcrystal (–40°C); E — brittle fracture of transcrystal and intercrystal character (in the middle of the weld metal) (–60°C);F — transcrystal brittle fracture with the presence of micro openings (in the middle of the weld metal)(–60°C).

of a minimal thickness (9.5 mm) has the finest structure and a satisfactory homogeneity in the cross sections of samples.

The appearance of weld metal microstructure at characteristic places in the welded joints can be seen in Fig. 1A–F. The presence of different morphological forms of ferrite was noticed in the weld metal structure of all samples. Mostly present were acicular ferrite (AF), ferrite with a secondary phase (FS), and Widmanstätten ferrite (WF).

For the samples welded with electrode N1 and with low heat input, the weld metal microstructure consisted of AF, in amounts to ~ 50% for the minimal thickness of steel strip. With the increase in and strip thickness, the share of AF was reduced and to ~ 35%, while the rest of the structure consisted of PF and FS separated along grain boundaries — Fig. 1A, B.

In the weld metal samples welded with electrode NM1, approximately 35% of AF was found (for the minimal thickness of steel strip, t_0 = 9.5 mm). With an increase in strip thickness, the amount of AF increased and reached ~ 50%, while the rest consisted of FS + SF — Fig. 1C–F.

By comparison of weld metal microstructures of both groups of tested samples with the expected microstructure, which would be derived from the appropriate CCT diagram, it can be concluded that satisfactory compliance has been achieved in terms of microstructure.

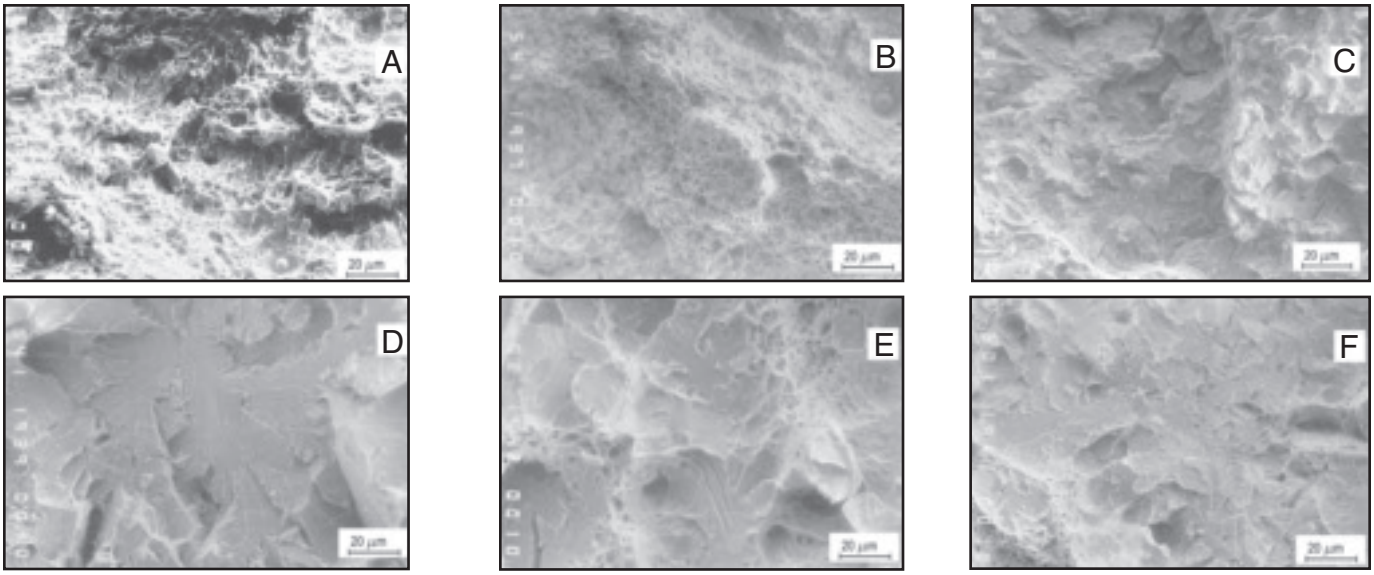

Fig. 7 — SEM, fracture surface of the weld metal made by using electrode NM1 on microalloyed steel X65 (quality E, t_1 = 11.0 mm). A, B — Ductile fracture (–20°C); C — brittle fracture of transcrystal and intercrystal character, (–40°C); D — brittle fracture caused by tearing (–40°C); E — brittle fracture of trans crystal and intercrystal character in the middle of the weld metal, (—60°C); F — brittle fracture in the middle of the weld metal (–60°C).

In the HAZ, changes in grain size were observed, as well as their growth toward the weld interface in the overheated zone where a coarse ferrite-bainite structure was formed with carbides arranged along boundaries of former austenite grains — Figs. 3–5.

The results of fractographic analysis after tests performed at temperatures of +20°, –40°, and –60°C are given in Figs. 6 and 7. Comparative analysis of these results indicated a better quality of weld metal structure when using electrode NM1 (1.4% Ni, 0.35% Mo) in relation to the weld metal structure when using electrode N1 (1.0 % Ni) at all test temperatures. The content of nickel and molybdenum in the filler metal, in addition to C and M, is significant for achieving the optimum ratio of structural components in the weld metal. Based on the analysis of measured values of tensile strength of the welded joints, it can be concluded that values are higher than the base metal (for steels D and E), and at the level of the base metal (for steel F) as shown in Fig. 8A and B.

Analysis of the results of hardness testing showed that an increased number of passes had an impact on lowering weld metal hardness (as measured at the middle of the height of the weld metal) — Fig. 9A–C. Results of impact toughness testing of welded joints showed that higher toughness values at lower temperatures were achieved with electrode NM1 — Fig. 10A–C.

Conclusions

Based on the experimental results obtained by examining the impact of filler metal quality and welding parameters on the structural change in the weld metal and HAZ of microalloyed X65 steel, the following conclusions were made:

1) Addition of Ni into the weld metal with the filler metal marked N1 (1.0% Ni) improved the formation of acicular ferrite, while the addition of Ni and Mo with the filler metal marked NM1 (1.4% Ni, 0.35% Mo) had an effect on achieving the optimum ratio of structural components (AF + PF, FS).

2) In the weld metal for electrode NM1 (steel strip thickness t_2 = 14.5 mm, heat input E_2 = 16.8 kJ/cm, electrode NM1), the AF amount was over 50% in the last pass, and the rest consisted of PF and FS. The same proportion of AF was achieved in the weld metal when using electrode N1 (steel strip of minimum thickness t_0 = 9.5 mm and heat input E_1 = 6.8 kJ/cm).

3) Microstructural analysis of the HAZ of welded joints obtained with different levels of heat input (E_1 = 13.7 kJ/cm and E_2 = 16.5 kJ/cm) showed that the structure was finer with a lower level of heat input in the normalizing and overheated zone.

4) Fractographic analysis of the fracture surface of the weld metal obtained by using electrode NM1 at +20°C shows ductile fracture. On specimens tested at –40°C, a mixed fracture with a large share of transcrystal fracture was observed. At –60°C, a brittle fracture is evident of transcrystal and intercrystal character.

5) In microalloyed X65 steel, the best quality of welded joints was achieved with electrode NM1 and a heat input of 13.7 to 16.5 kJ/cm.

6) The test results for mechanical properties of welded joints confirmed the re-

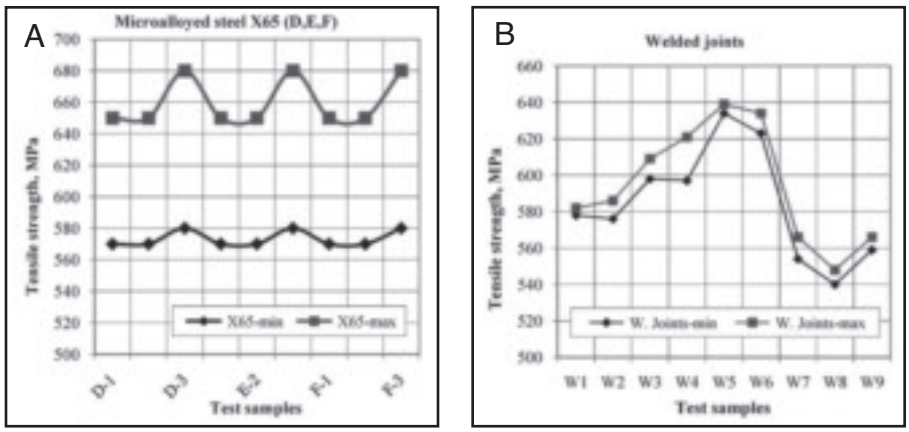

Fig. 8 — Tensile strength. A — Base metal, microalloyed steel X65; B — welded joints:
W1 (D-N1/E_1 = 6.8 kJ/cm, 6 passes)
W2 (D-N1/E_2 = 12.3 kJ/cm, 9 passes)
W3 (D-NM1/E_3 = 16.8 kJ/cm, 5 passes)
W4 (E-N1/E_1 = 7.3 kJ/cm, 9 passes)
W5 (E-N1/E_2 = 9.2 kJ/cm, 9 passes)
W6 (E-NM1/E_3 = 13.7 kJ/cm, 5passes)
W7 (F-N1/E_1 = 9.1 kJ/cm, 10 passes)
W8 (F-N1/E_2 = 10.8 kJ/cm, 4 passes)
W9 (F-NM1/E_3 = 16.6 kJ/cm, 7 passes)

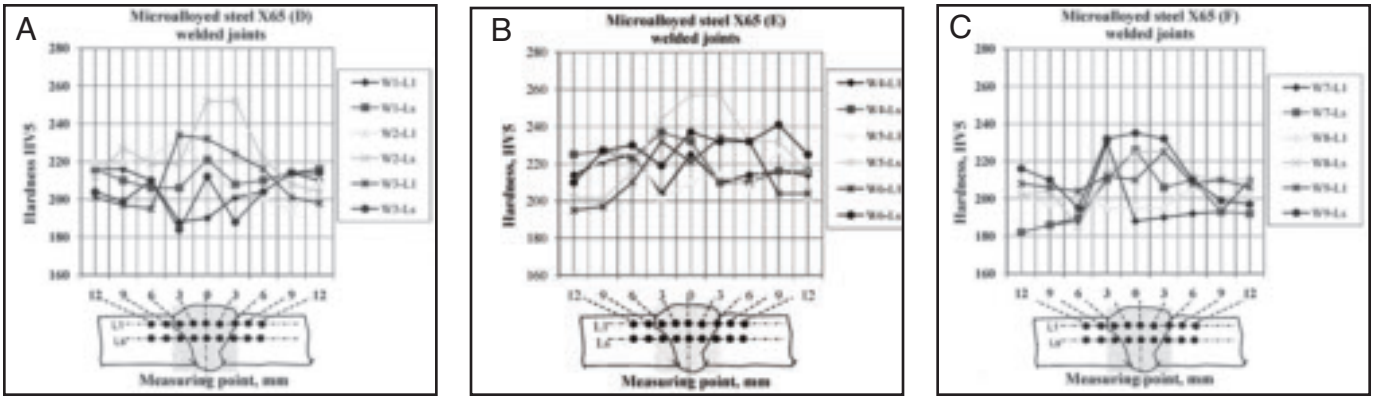

Fig. 9 — Change of hardness in the cross section of welded joints. A — W1 (D-N1/E_1 = 6.8 kJ/cm, 6 passes), W2 (D-N1/E_2 = 12.3 kJ/cm, 9 passes), W3 (D-NM1/E_3 = 16.8 kJ/cm, 5 passes); B — W4 (E-N1/E_1 = 7.3 kJ/cm, 9 passes), W5 (E-N1/E_2 = 9.2 kJ/cm, 9 passes), W6 (E-NM1/E_3 = 13.7 kJ/cm, 5 passes); C — W7 (F- N1/E_1 = 9.1 kJ/cm, 10 passes), W8 (F-N1/E_2 = 10.8 kJ/cm, 4 passes), W9 (F-NM1/E_3 = 16.6 kJ/cm, 7 passes).

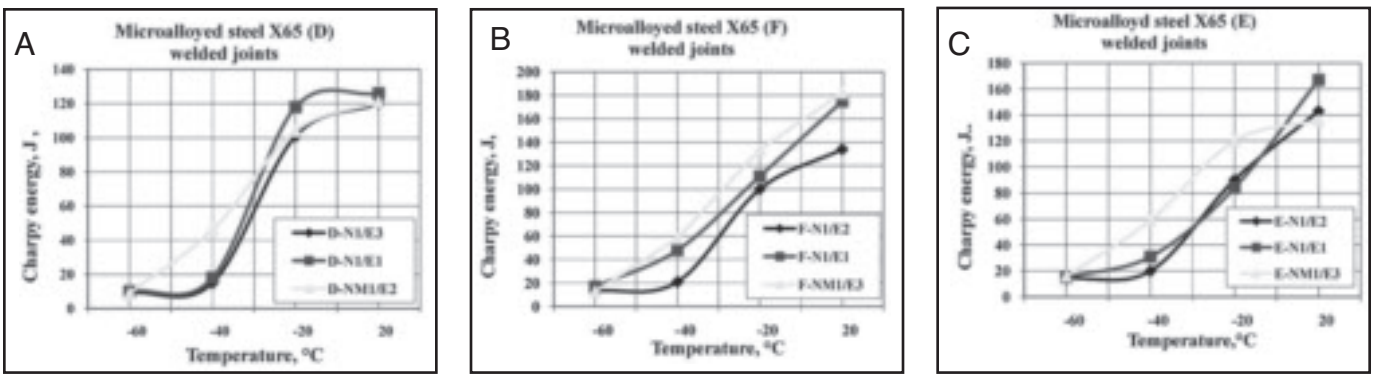

Fig. 10 — Impact toughness of weld metal depending on test temperature. A — D (N1/E_1 = 6.8 kJ/cm, N1/E_2 = 12.3 kJ/cm i NM1/E_3 = 16.8 kJ/cm); B — E (N1/E_1 = 7.3 kJ/cm, N1/E_2 = 9.2 kJ/cm i NM1/E_3 = 13.7 kJ/cm); C — F (N1/E_1 = 9.1 kJ/cm, N1/E_2 = 10.8 kJ/cm i NM1/E_3 = 16.6 kJ/cm)

sults of metallographic examinations. Welded joints with better characteristics were obtained with the electrode NM1.

Acknowledgments

This work was supported by the Serbian Ministry of Science and Technological Development (project number 19061).

References

1. Bajic, N., and Sijacki-Zeravcic, V. 2003. *Welding and Welded Structures*, Vol. 3, p. 5.

2. Bajic, N., Sijacki-Zeravcic, V., Rakin, M., and Kovacevic, K. 2005. Structure optimization of weld metal and HAZ in microalloyed high-strength steel welded joints. *YUCOMAT 2005*, Herceg Novi, (SBN: 86-80321-08-7), pp. 193–200.

3. Radovic, A., Bajic, N., and Grabulov, V. 1996. Specific quality of the weld metal of welded joints of fine-grained microalloyed steels. *Zavarivanje 96*, Belgrade, pp. 61–72 (in Serbian).

4. Bajic, N. 2004. Analysis of the filler material and welding parameters influence on properties of weld joints of new generation of high-strength microalloyed steels, (in Serbian). PhD dissertation, Faculty of Mechanical Engineering, Belgrade.

5. Mitchell, P. S., Hart Mand, P. H., and Morrison, W. B. 1995. The effect of microalloying on HAZ toughness. *Microalloying*, Pittsburgh, Pa., pp. 149–162.

6. Zhang, Z., and Farrar, R. A. 1995. An atlas of continuous cooling transformation (CCT) diagrams applicable to low-carbon low-alloy weld metals. *Met. B5*, The Institute of Materials, London, UK.

7. Osama, A. K. 1985. Weld metallurgical aspects and crack sucseptibility in high-strength steels: weldability of materials and testing methods. *Vranje*, pp. 49–57.

8. Bhadeshija, H. K. D. 1992. *Bainite in Steels*. The Institute of Materials, London, UK, pp. 45–58.

9. Li, Y., Crowther, D. N., Green, M. J. W., and Mitchell, P. S. 2001. The effect of vanadium and niobium on the properties and microstructure of the intercritically reheated coarse-grained heat-affected zone in low-carbon micro-alloyed steels. *ISIJ International*, Vol. 41, pp. 46–61.

10. Evans, G. M. 1990. The effect of alloying elements on the microstructure and properties of ferrite all-weld-metal deposits. *Welding-90*, Zurich, Switzerland.

11. Evans, G. M. 1989. The effect of nickel on the properties of C-Mn as-welded metal deposits (I.I.W2-1A-791-89).

12. Hallen, G. 1984. Some aspects on the formation of microstructure in multipass welds in ferritic ductile iron. *3rd Int. Symp. on the Physical Metallurgy of Cast Irons*, Stockholm, Sweden, pp. 457–65.

13. Bernard, G. A. 1977. Viewpoint on the weldability of carbon-manganese and microalloyed structural steels. *Microalloying 75, Proceedings of an International Symposium on High-Strength, Low-Alloy Steels*. New York, N.Y., pp. 552–566.